

Fig. 1. ^RQ₇, ^RR₆ and ^RQ₉ manifolds structure of the ν_6 band between 936 and 958 cm⁻¹ in spectrum 3 (see experimental conditions in Table 1).

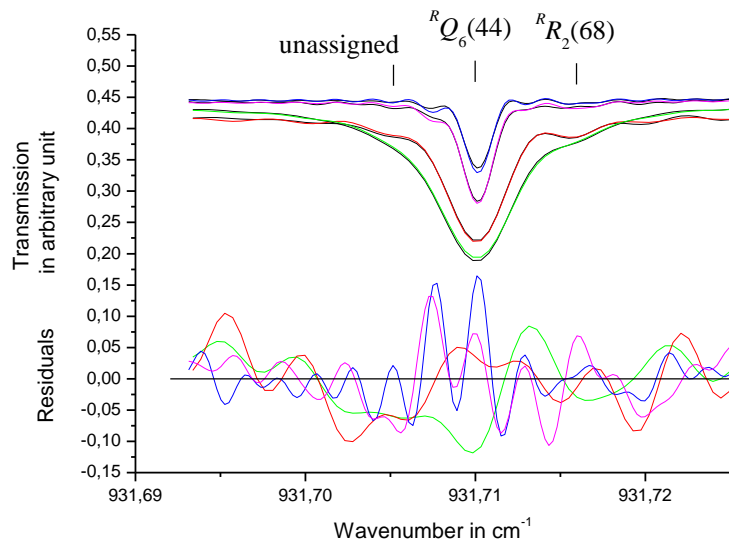


Fig. 2. Multispectrum fit of 3 transitions in spectra 1-4 (see Table 1 for experimental conditions). Residuals are printed as $(\text{Obs}-\text{Calc})/\text{Calc} \times 10$ so that a deviation of 0.1 in the vertical scale corresponds to a residual of 1%.

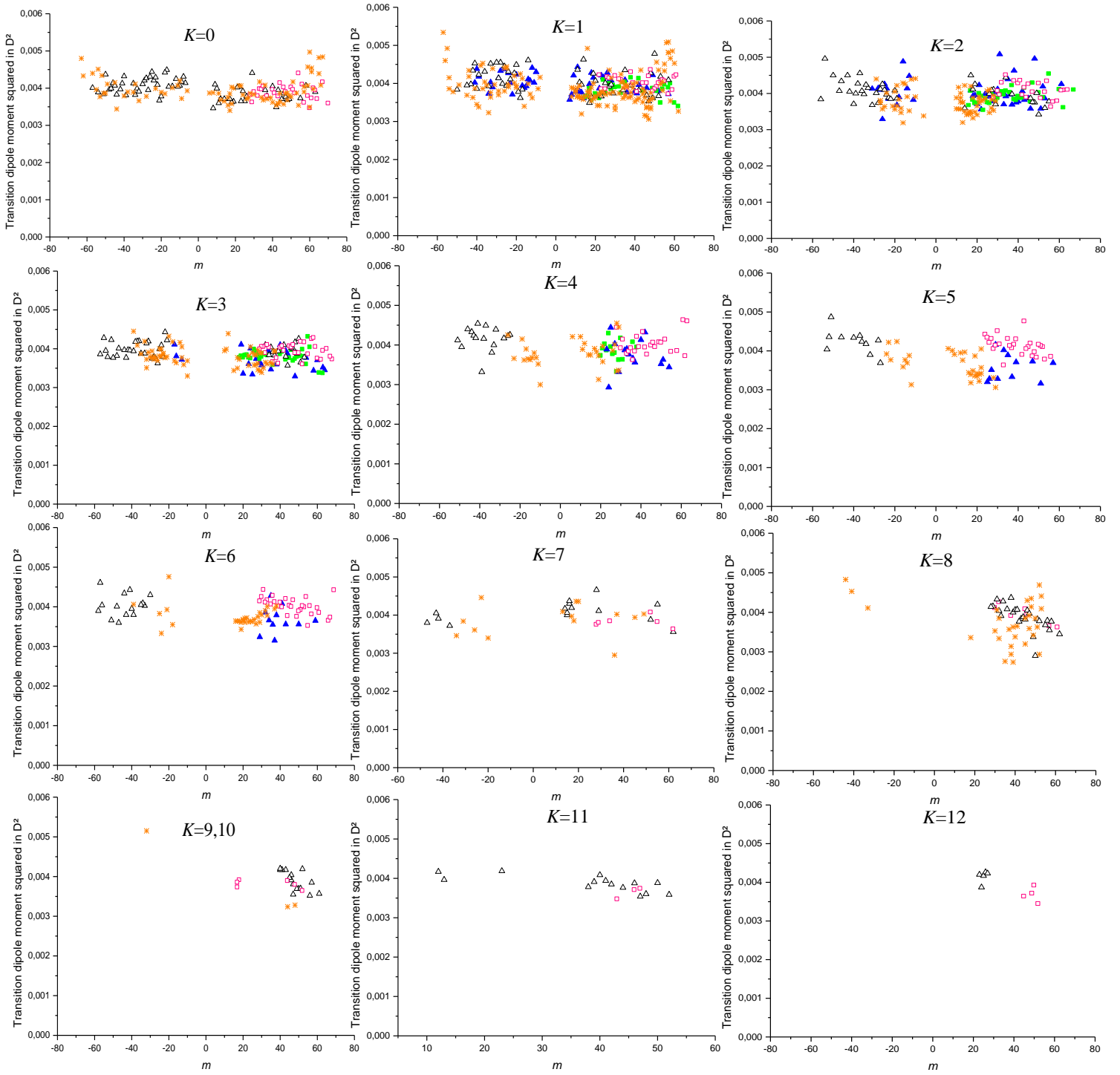


Fig. 3. Transition dipole moment squared R^2 obtained (using Eqs. (2-4)) from line intensity measurements of this work and Ref. [13] for $K=0$ to 12. The experimental measurements are plotted using following symbols: black open triangles for ${}^R P$ and ${}^R R$ sub-branches, blue solid triangles for ${}^P P$ and ${}^P R$ sub-branches, pink open squares for ${}^R Q$ sub-branch and green solid squares for ${}^P Q$ sub-branches. The orange stars corresponds to calculation of transition dipole moment squared using measurements of Ref. [13].

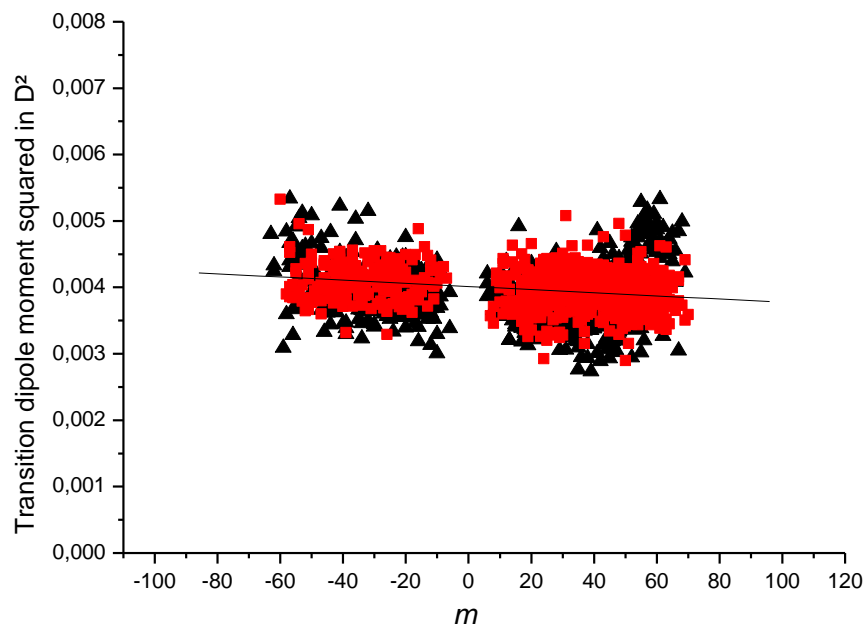


Fig. 4: Transition dipole moment squared for all line intensities measured in this work (red squares) and in Ref. [13] (black triangles). The continuous line represent the calculated transition dipole moment squared using Eq. (4) and R_0^2 and A parameters obtained in this work (see text).

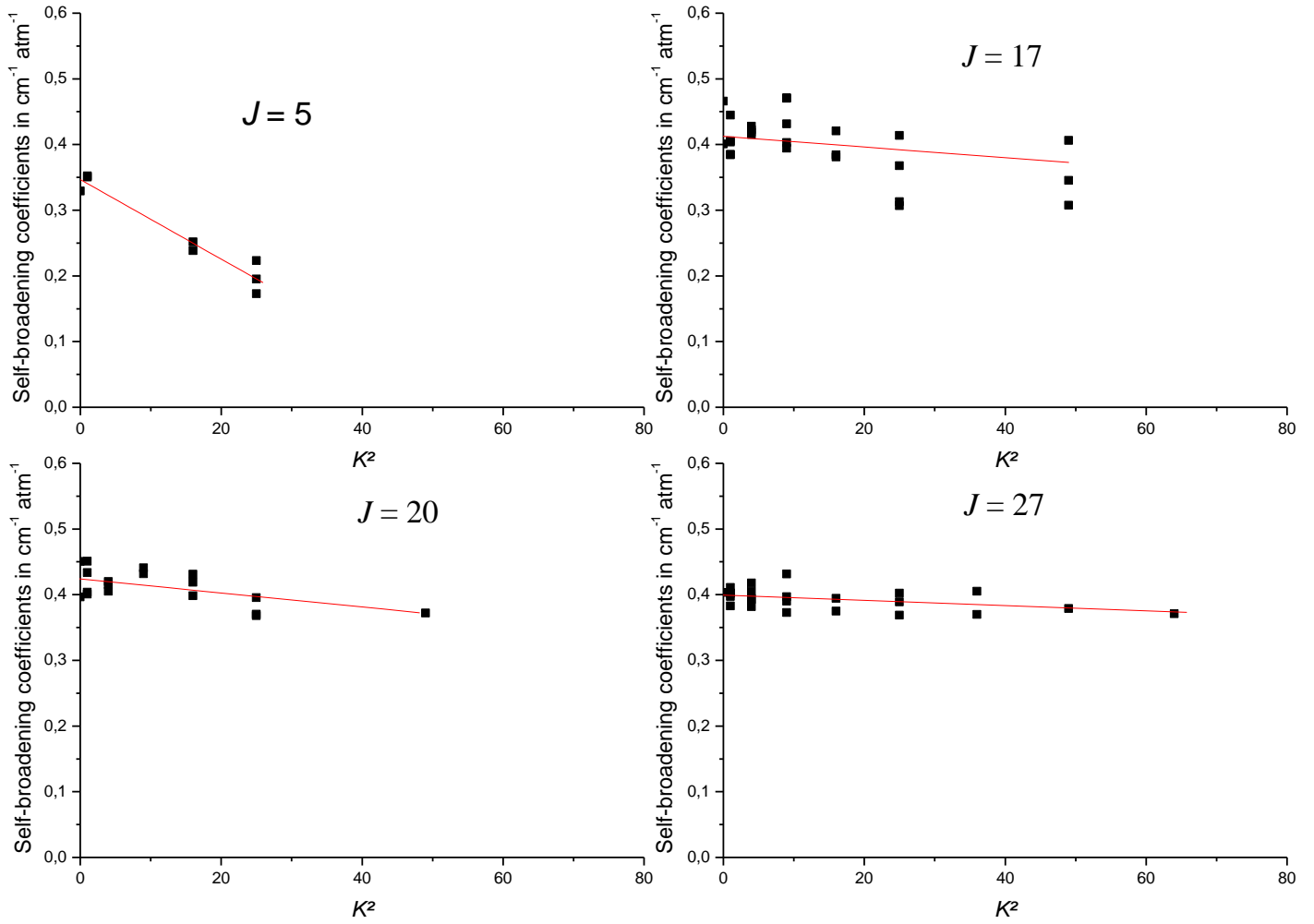


Fig. 5. K -rotational dependences of the measured self-broadening coefficients for four J values ($J = 5, 17, 20$ and 27). The solid symbols represent the measured self-broadening coefficients used to retrieve the a_j^0 and a_j^2 parameters of Eq. (5). The continuous red line corresponds to the modeled widths using Eq. (5) and parameters of Table 4.

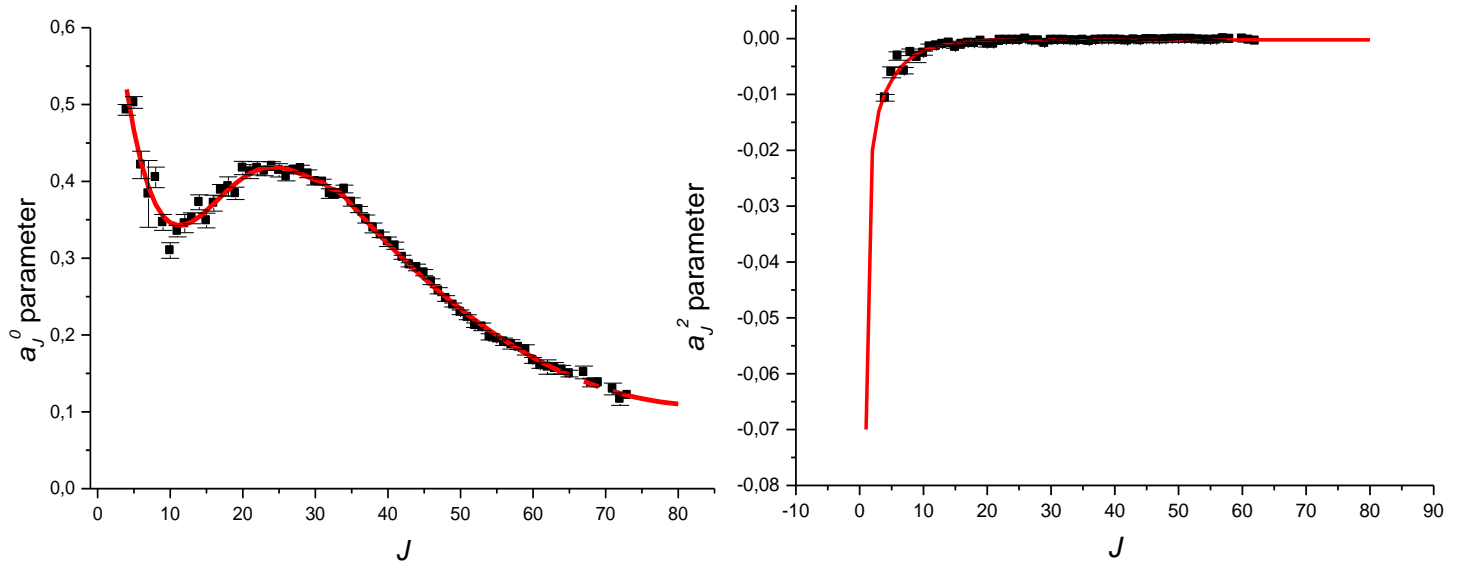


Fig. 6. Parameters a_J^0 and a_J^2 (in $\text{cm}^{-1} \cdot \text{atm}^{-1}$) deduced from the fit of the measured self-broadening coefficients using Eq. (5). The continuous line represents the values calculated by Eq. (5) using smoothed parameters of Table 4. Error bars associated to the fitted a_J^0 and a_J^2 parameters correspond to the RMS of the fit (1SD).

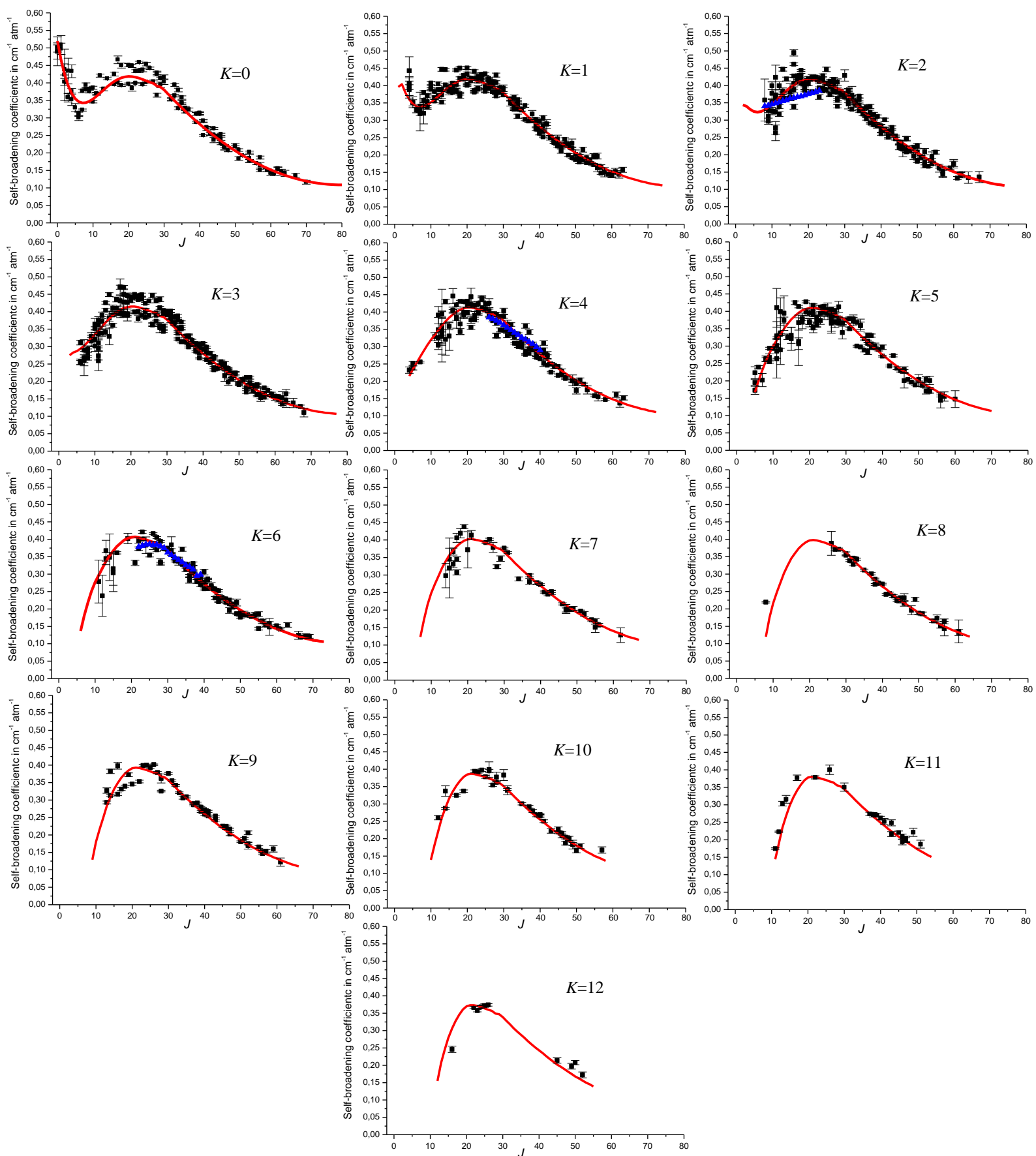


Fig. 7. J - and K -dependences of measured and calculated self-broadening coefficients of CH_3I . Solid black squares represent the measured line widths from this work. Continuous lines correspond to values resulting from Eq. (5) and smoothed parameters of Table 4. Solid blue triangles represent the measured self-broadening coefficient from Ref. [26]. Error bars associated to the measurements correspond to the SD of the fit.

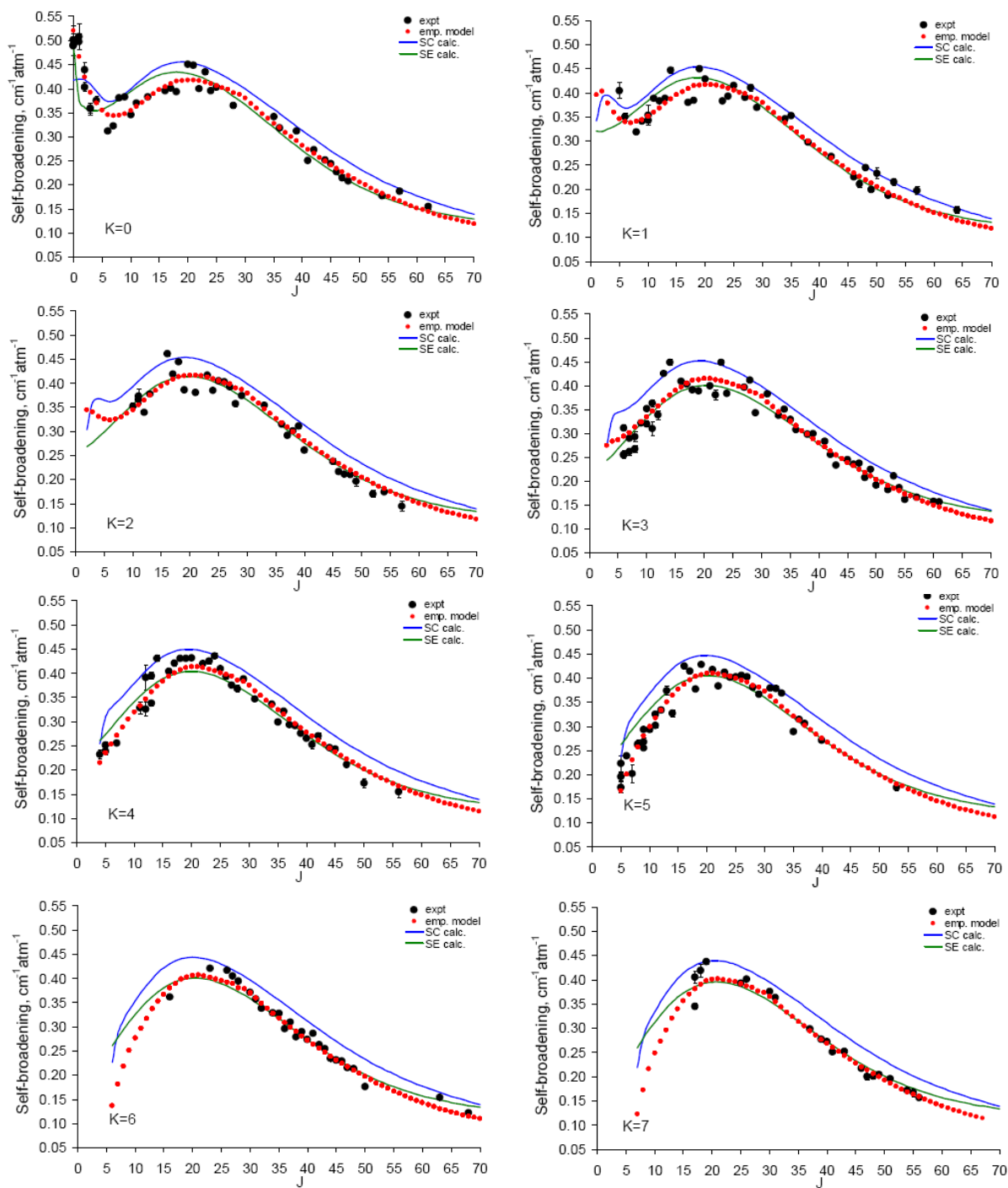


Fig. 8. Comparison of experimental, empirical and theoretical (semi-classical SC and semi-empirical SE) J -dependences of room-temperature CH_3I self-broadening coefficients at various K values for the $^R R$ -sub-branch of the ν_6 band.

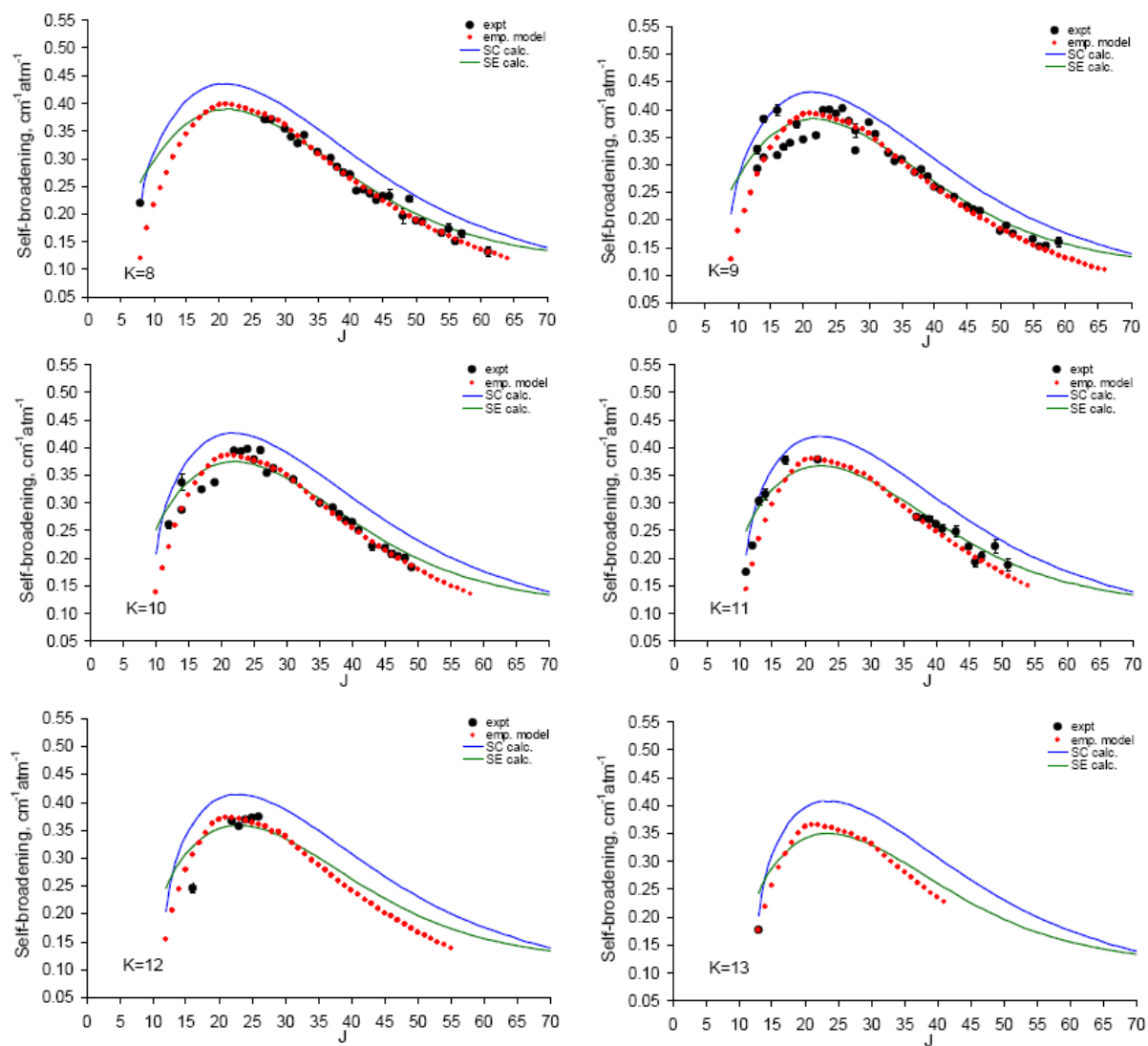


Fig. 8. Continued.

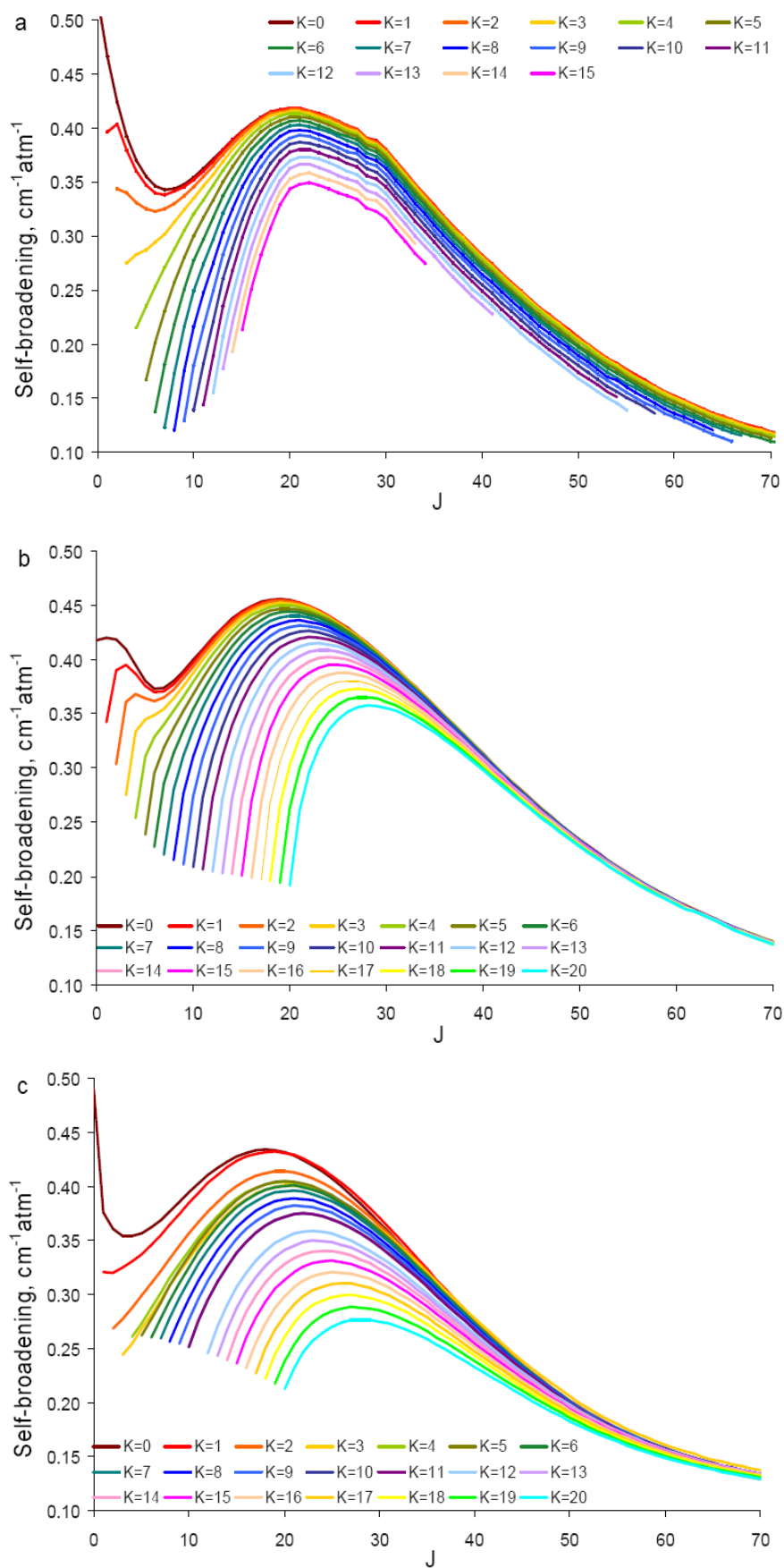


Fig. 9. Comparison of empirical (a), semi-classical (b) and semi-empirical (c) J -dependences of room-temperature CH_3I self-broadening coefficients at various K values for the $^R R$ -sub-branch of the ν_6 band.